Lipid rafts sense and direct electric field-induced migration

Bo-jian Lin (林柏江)[a], Shun-hao Tsao[a], Alex Chen[b], Shu-Kai Hu[b], Ling Chao (趙玲)[b], and Pen-hsiu Grace Chao (趙本秀)[a,1]

[a]Institute of Biomedical Engineering, School of Medicine and School of Engineering, National Taiwan University, Taipei 106, Taiwan; and [b]Department of Chemical Engineering, School of Engineering, National Taiwan University, Taipei 106, Taiwan

Edited by Shu Chien, University of California, San Diego, La Jolla, CA, and approved June 30, 2017 (received for review February 18, 2017)

Endogenous electric fields (EFs) are involved in developmental regulation and wound healing. Although the phenomenon is known for more than a century, it is not clear how cells perceive the external EF. Membrane proteins, responding to electrophoretic and electroosmotic forces, have long been proposed as the sensing molecules. However, specific charge modification of surface proteins did not change cell migration motility nor directionality in EFs. Moreover, symmetric alternating current (AC) EF directs cell migration in a frequency-dependent manner. Due to their charge and ability to coalesce, glycolipids are therefore the likely primary EF sensor driving polarization of membrane proteins and intracellular signaling. We demonstrate that detergent-resistant membrane nanodomains, also known as lipid rafts, are the primary response element in EF sensing. The clustering and activation of caveolin and signaling proteins further stabilize raft structure and feed-forward downstream signaling events, such as rho and PI3K activation. Theoretical modeling supports the experimental results and predicts AC frequency-dependent cell and raft migration. Our results establish a fundamental mechanism for cell electrosensing and provide a role in lipid raft mechanotransduction.

electric field | migration | lipid raft | caveolin | integrin

During development and wound healing, cells experience electrical currents (1–3). The electric field (EF) results in polarized cell organization and induces directional cell migration (galvanotaxis or electrotaxis), morphological changes (galvanotropism), and alterations in gene expression (4, 5). In development, the electrical currents arise from regulation of ion channels that lead to ion flux and establish polarization and morphogenesis (1, 6). EF is also generated from the disruption of membrane potentials at wound sites and promotes oriented cell division and migration, facilitating wound healing (7, 8). Suppression of the electrical currents can lead to impaired healing and failed development (9, 10).

How do cells perceive the external EFs? As the plasma membrane consists of mostly negatively charged molecules that move in the plane of the membrane, the external field induces electrophoresis and electroosmosis of these molecules (11–13). A number of membrane proteins have been found to polarize in direct current (DC) EF, including acetyl choline receptors, VEGF/EGF receptors, and integrins (14–17). In addition, electrical stimulations are found to regulate ion channel activities with higher activation toward the cathode (18). Through these polarized surface receptors, the external EFs activate intracellular signaling, such as src kinase (src), small GTPases, and phosphoinositol kinase pathways, which are polarized in the EF-induced migration direction (7, 17).

Although the preferential distribution and activation of cell membrane proteins in EF support the notion that charged cell surface molecules are influenced by the electrophoretic and electroosmotic forces, Finkelstein et al. (19) report that modification of membrane protein charges with avidin conjugation does not change cell migration motility nor directionality in EF. Interestingly, the classical neurominidase treatment, which removes sialic acids from both glycoproteins and glycolipids, indeed inhibits directional migration. These results suggest that glycolipid redistribution in EF can be an alternative candidate as the primary EF sensor in cell membrane. Moreover, we previously reported that symmetric alternating current (AC) at 50 Hz drives directional cell migration (17). Glycolipids are capable of congregating into structures such as lipid rafts that can increase in size by recruiting proteins and lipids. EFs may induce glycolipid movement and density increase due to preferential distribution in the field, leading to increases in lipid raft size (20). If raft size increases during movement in EF, the concomitant decrease in raft motility will result in polarization of the raft structures and lead to directional migration.

Lipid rafts, detergent-resistant membrane nanodomains, are highly dynamic and heterogeneous in composition and interaction (21). They are essential in many cell membrane processes and modulate activation of integrin and many of the aforementioned growth factor receptors that polarize in EF (22–24). Rich in gangliosides, lipid rafts are linked to sialic acids and negatively charged. In addition to cholesterol, lipid raft proteins, such as caveolin (Cav), further stabilize lipid raft structure and control lipid raft dynamics (25, 26). In the current study, we hypothesize that lipid rafts are the primary sensor to EF stimulation due to their charge and ability to coalesce. Preferential distribution of lipid rafts in EF polarizes membrane proteins such as integrin and Cav, and the clustering and activation of these proteins further stabilize raft structure and feed-forward raft polarization, leading to directional cell migration.

Results and Discussion

We quantified the distribution of lipid rafts upon field exposure with fluorescent cholera toxin B (CTxB) to confirm the

Significance

Electric fields control embryonic development and wound healing through directing and enhancing cell migration and proliferation. However, details pertaining to electric sensing of cells remain unclear. Many studies have reported involvement of different cell surface proteins, yet the identity of the electric field sensor is unknown. We demonstrate that the detergent-resistant membrane nanodomains, known as lipid rafts, act as the primary sensor to electric field-induced directional cell migration. These nanodomains respond to electric fields as mobile complexes that polarize, coalesce, and partition membrane proteins and in turn activate intracellular signaling events to orient cell migration.

Author contributions: B.-j.L. and P.-h.G.C. designed research; B.-j.L., S.-h.T., A.C., S.-K.H., L.C., and P.-h.G.C. performed research; L.C. and P.-h.G.C. contributed new reagents/analytic tools; B.-j.L., S.-h.T., and P.-h.G.C. analyzed data; and L.C. and P.-h.G.C. wrote the paper.

The authors declare no conflict of interest.

This article is a PNAS Direct Submission.

[1]To whom correspondence should be addressed. Email: pgchao@ntu.edu.tw.

This article contains supporting information online at www.pnas.org/lookup/suppl/doi:10.1073/pnas.1702526114/-/DCSupplemental.

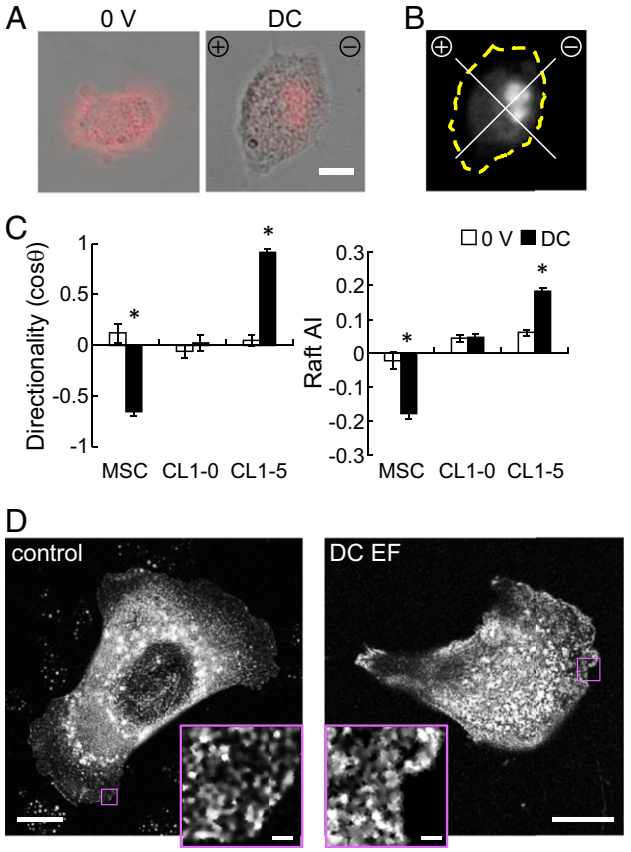

Fig. 1. Applied EF directs cell migration and lipid raft polarization. (*A*) Sample lipid raft labeling with CtxB. (Scale bar, 10 μm.) (*B*) Schematic for AI calculation, which was calculated as the difference of normalized fluorescent intensity between the region toward the cathode and the anode. (*C*) Galvanotactic behaviors of hMSC, CL1-0, and CL1-5 cells, and lipid raft distribution after 1 h of exposure to DC EF (n = 51–265, *P < 0.0001 vs. 0 V). (*D*) Superresolution microscopy images of representative cells labeled with CTxB for lipid raft. [Scale bar, 10 μm and (*Inset*) 1 μm.]

polarization of lipid rafts in applied DC and AC EFs. In DC fields, lipid rafts indeed polarized toward the cathode with time, corresponding with the migration directionality of fibroblasts and mesenchymal stem cells (MSCs) (Fig. 1 and *SI Appendix*, Fig. S1). In the anodally migrating CL1-5 adenocarcinoma cells, rafts were polarized toward the anode (27) (Fig. 1*C*). In the randomly migrating CL1-0 cells, no preferential raft distribution was found. Superresolution microscopy revealed a significant increase of raft sizes with DC EF exposure in MSCs, indicative of raft clustering (control = 0.028 ± 0.005 μm^2, EF = 0.032 ± 0.007 μm^2, n = 19–24, P = 0.014; Fig. 1*D*). When lipid rafts were disrupted by cholesterol depletion with methyl β-cyclodextrin (MβCD) or saturation, migration directionality was suppressed, whereas the influence on motility, as quantified by migration speed, was minor (Fig. 2). These data support our hypothesis that EF-induced migration directionality corresponds with membrane raft clustering and polarization.

We previously reported that integrin mediates directional cell migration in applied EFs (17). The polarized distribution of integrin in response to EF was abolished with raft disruption, whereas raft polarization in EF was less influenced by functional blocking of integrin (Fig. 3*A*). To further determine if lipid rafts indeed act upstream of integrin or other active cellular mechanisms, we disrupted the actin cytoskeleton with cytochalasin D to monitor raft distribution. Although cytochalasin treatment

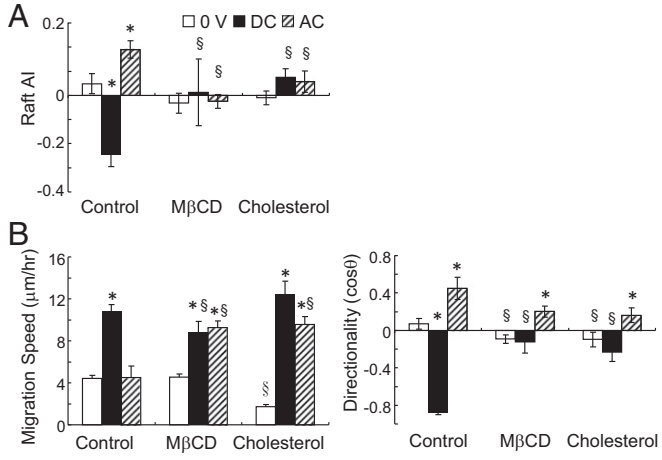

Fig. 2. Lipid raft polarization in applied AC and DC fields. Manipulation of raft with MβCD and cholesterol-suppressed raft polarization (*A*) and directed cell migration (*B*). (*A*) n = 17–188, *P < 0.05 vs. 0 V, §P < 0.03 vs. control. (*B*) n = 25–171, *P < 0.02 vs. 0 V, §P < 0.05 vs. control.

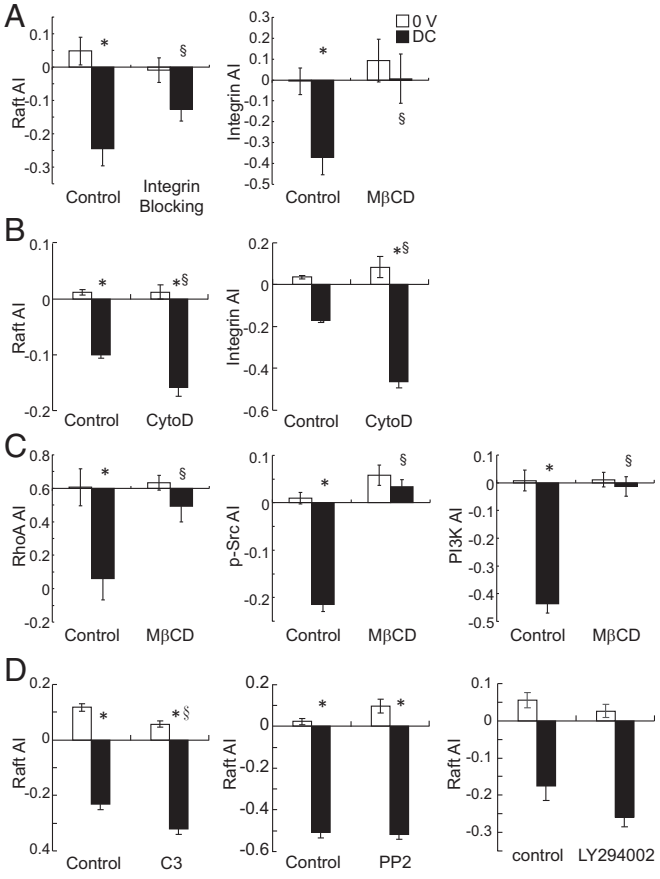

Fig. 3. Lipid rafts act upstream of intracellular structure and signaling mechanisms. (*A*) Integrin blocking partially suppressed lipid raft polarization in response to applied EF, whereas lipid raft disruption diminished integrin polarization in EF (n = 32–58, *P < 0.005 vs. 0 V, §P < 0.05 vs. control). (*B*) Actin cytoskeleton disruption enhanced polarized lipid raft and integrin distribution in EF (n = 20–262, *P < 0.0001 vs. 0 V, §P < 0.0001 vs. control). (*C*) Lipid raft disruption attenuated polarized RhoA, Src, and PI3K distribution (n = 4–73, *P < 0.01 vs. 0 V, §P < 0.02 vs. control), whereas (*D*) RhoA, Src, or PI3K inhibition (with C3 exoenzyme, PP2, and LY294002, respectively) did not suppress lipid raft redistribution (n = 70–127, *P < 0.0001 vs. 0 V, §P < 0.001 vs. control).

CELL BIOLOGY

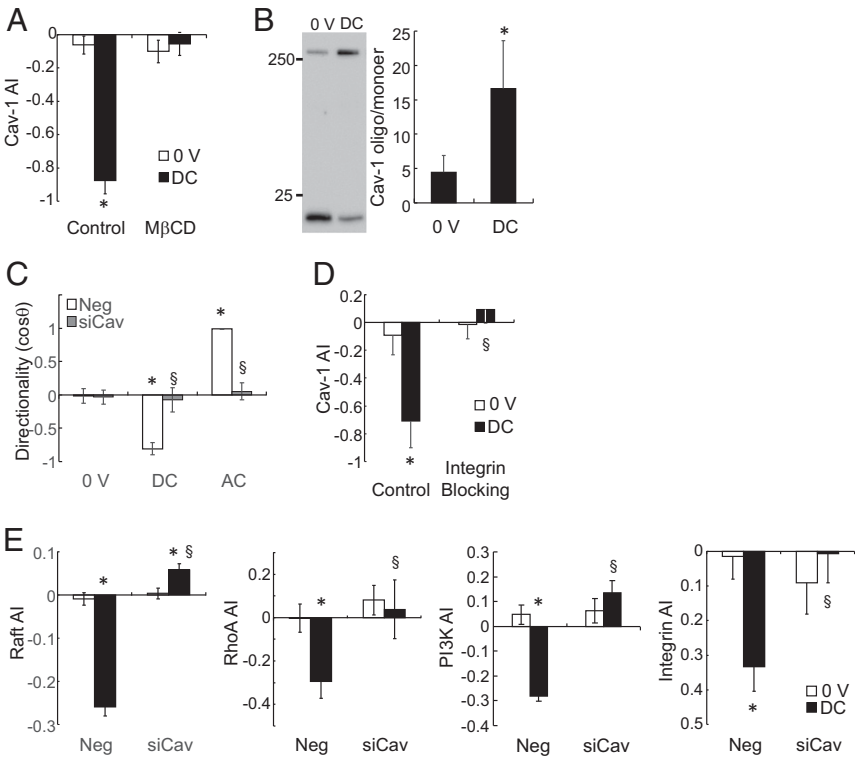

Fig. 4. Applied EF polarizes and clusters Cav for directional migration. (*A*) Lipid raft disruption inhibited Cav-1 polarization in EF (n = 26–42, *P < 0.001 vs. 0 V, §P < 0.001 vs. control). (*B*) EF induced Cav oligomerization (P < 0.05, n = 5). (*C*) Cav knockdown reduced EF-induced directional migration (n = 11–46, *P < 0.0001 vs. 0 V, §P < 0.003 vs. neg). (*D*) Functional blocking of integrin suppressed polarized distribution of Cav (n = 14–42, *P < 0.01 vs. 0 V, §P < 0.0001 vs. control). (*E*) Cav-1 knockdown attenuated raft, RhoA, PI3K, and integrin polarization in response to applied EF (n = 13–107, *P < 0.03 vs. 0 V, §P < 0.02 vs. neg).

significantly suppressed cell motility and directionality (*SI Appendix*, Fig. S1*B*), actin disruption enhanced raft and integrin polarization (Fig. 3*B*). In addition, no preferential lamellipodia extension toward the cathode (*SI Appendix*, Fig. S1*A*) or microtubule organizing center polarization (28) was found with EF exposure. As cytoskeleton structures, especially actin, regulate membrane domains and protein organization (29, 30), the increase of raft polarization with cytochalasin treatment supports the restrictive role of submembranous cytoskeleton structures in the diffusion of membrane proteins (31).

To understand the interaction between integrin and lipid raft, dual labeling with CTxB and antibody against active β1 integrin (clone 12G10, Abcam) found no changes in raft and integrin colocalization after EF stimulation (P = 0.775; *SI Appendix*, Fig. S1*C*). Due to the pentavalent nature of CTxB, we tested the effects of CTxB on raft size and integrin interactions by treating the control cells with CTxB before formalin fixation. Indeed, CTxB treatment increased raft size by 15% (CTxB incubation after fixation, 0.028 ± 0.005 μm^2; CTxB incubation before fixation, 0.032 ± 0.007 μm^2, P = 0.039) and reduced integrin and raft colocalization by 36% (CTxB incubation after fixation, 0.242 ± 0.090; CTxB incubation before fixation, 0.156 ± 0.103, P = 0.019). As both CTxB and formalin fixation can artificially induce raft clustering (32), the reported raft size and colocalization may not reflect the actual values. Nonetheless, our results demonstrate that both CTxB and electrical stimulation increase raft clustering. Furthermore, EF-induced clustering has a different effect on integrin partitioning from the chemically induced clustering. These data suggest that EF may play an additional role in integrin and raft interaction, and integrin is not merely a passive passenger on the raft during EF-induced raft clustering. Clustering and activation of other molecules may also participate in the dynamics. Future studies should determine if inactive integrin association with raft, the ratio of active/inactive integrins, or recruitment of different integrin species change with EF-induced raft clustering. Our results demonstrate that exogenous EF alters raft and integrin interactions.

Polarization of intracellular signaling molecules, including RhoA, src, and PI3K, mediates EF-induced directionality (7, 17). To understand the role of raft in the polarization of these downstream factors, we examined their distribution in applied EF after raft disruption and found polarization of these signaling proteins was abolished (Fig. 3*C*). Pharmacological inhibition of these molecules, on the other hand, had no effect on lipid raft polarization in EF (Fig. 3*D* and *SI Appendix*, Fig. S2), further demonstrating that lipid raft polarization acted upstream of these intracellular signaling events.

An integral inner membrane protein, Cav stabilizes lipid raft structures and interacts with β_1 integrin to activate RhoA through inactivation of p190RhoGTPase (33). In applied DC EF, Cav-1 polarized toward the cathode, similar to the gangliosides of lipid raft (Fig. 4*A*). EF stimulation for 1 h significantly increased Cav oligomerization (Fig. 4*B*), indicating a clustering effect in response to the applied EF. Cholesterol depletion with MβCD inhibited Cav-1 polarization (Fig. 4*A*). Knockdown of Cav-1 abolished migration directionality in response to applied EF (Fig. 4*C*). As Cav regulates membrane cholesterol content (34), we replenished membrane cholesterol in the Cav-1 knockdown cells and found a similar suppression of directionality, indicating that Cav indeed participated in EF-induced raft redistribution (*SI Appendix*, Fig. S3). Cav-1 knockdown also inhibited RhoA and PI3K polarization in EF, demonstrating the key role of Cav-1 in EF-induced directional signaling (Fig. 4*E*). Interestingly, although inhibitors for PI3K and src did not

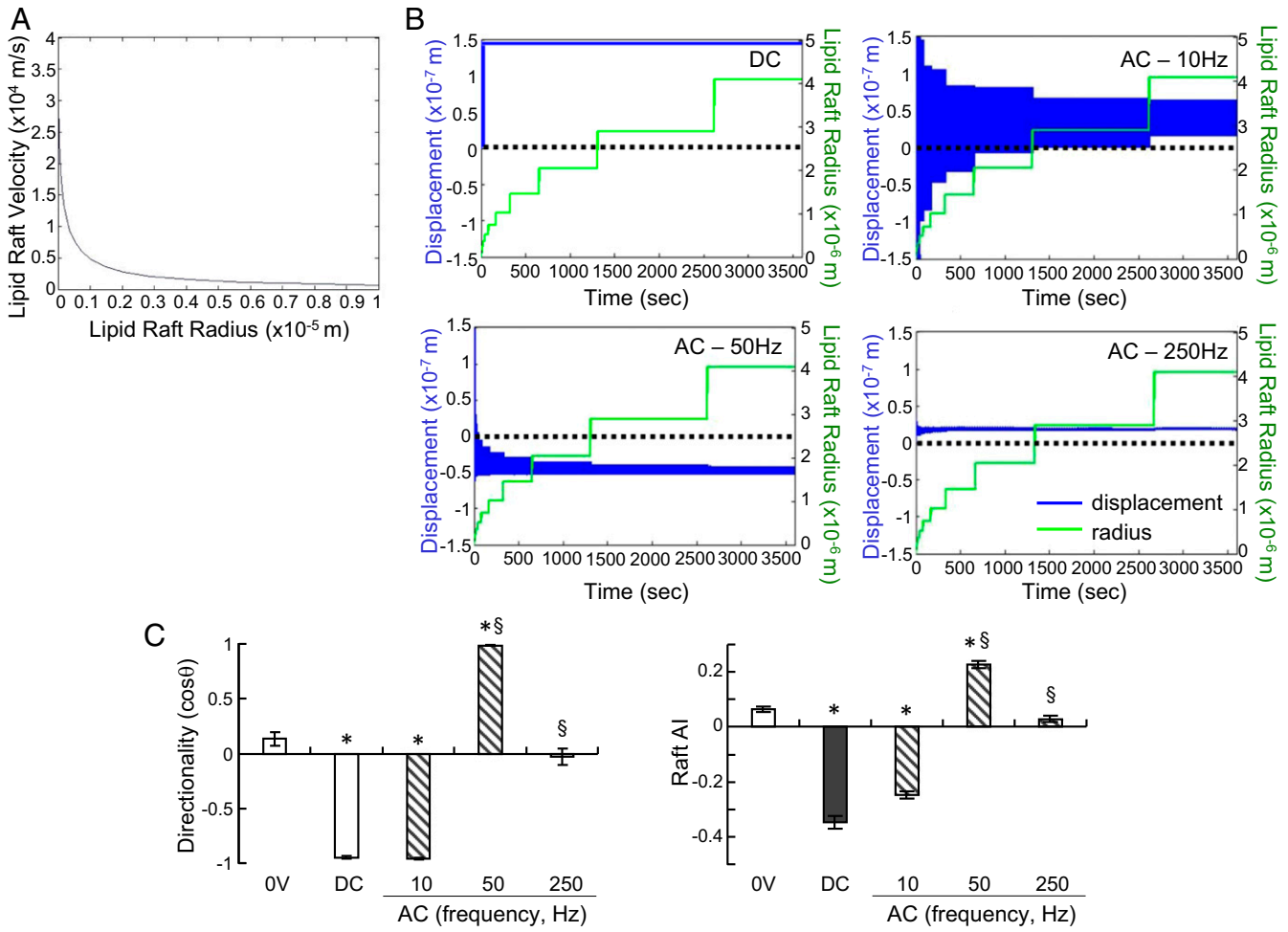

Fig. 5. Theoretical model of lipid raft movement in applied EF. (*A*) Lipid raft velocity as a function of lipid raft radius (0–10 μm) in an EF. (*B*) Model prediction of lipid raft displacement when the EF is applied as DC and AC field at 10 Hz, 50 Hz, or 250 Hz. Blue line and the left *y* axis, displacement of a lipid raft (x). Green line and the right axis, lipid raft radius (r). Dashed line, original location of lipid raft (x = 0). (*C*) DC and AC frequency-dependent response of lipid rafts and migration directionality of fibroblasts (n = 58–178, $^{*}P < 0.0001$ vs. 0 V, $^{\S}P < 0.0001$ vs. DC).

suppress Cav polarization in EF, functional blocking of integrin reduced Cav polarization (Fig. 4*D* and *SI Appendix*, Fig. S2). Inhibition of raft and integrin polarization from Cav-1 knockdown cells suggested reciprocal interactions among raft, integrin, and Cav-1, and the integrity of all three components was necessary for EF-directed migration. Activation of integrin by extracellular matrix proteins has been shown to change integrin partitioning (35–37), stabilize lipid rafts (38), and modulate EF-induced motility and directionality (4, 39). Integrin activation may also induce src signaling that phosphorylates Cav (40). However, as the src-family inhibitor used in this study (PP2) acts on all known Cav kinases (src, fyn, and abl) (41, 42), Cav phosphorylation is unlikely to be involved in integrin and Cav association in EF. Furthermore, as PP2 has no effect on raft or Cav polarization (Fig. 3*D* and *SI Appendix*, Fig. S2), src does not mediate Cav interactions to stabilize lipid raft.

Stemming from the experimental observations, we built a theoretical framework based on previous models to describe the qualitative electrodynamic behavior of lipid rafts in membranes. The model calculated lipid raft displacement in DC and AC EFs based on parameters extracted in fibroblasts. Detailed analyses can be found in *SI Appendix*. The applied EF can induce three forces acting on lipid rafts (12, 43, 44): the electrical force due to an external EF (F_E) (45), the hydrodynamic force resulting from the aqueous medium (F_{HA}) (46), and the drag force in membrane (F_{DM}) (47). Drift velocity of lipid rafts was obtained by expressing F_E, F_{HA}, and F_{DM}. As illustrated in Fig. 5*A*, raft velocity decreased exponentially with increasing radius. Equilibrium location of lipid rafts was therefore determined by the rate of lipid raft size increases and EF-driven drifts. The direction of the field when lipid raft reached critical size (where its velocity approximates zero) governed the equilibrium location of the raft, predicting a frequency-dependent directionality of lipid raft distribution in DC and AC fields. Fig. 5*B* depicted that rafts were preferentially distributed toward the cathode in DC fields, confirming our experimental findings (Fig. 1). The model also predicted that while in AC fields, rafts would be located toward the cathode at low frequency (10 Hz), toward the anode at intermediate frequency (50 Hz), and exhibit low directionality at high frequency (250 Hz). Indeed, experimental results matched the finding and demonstrated that raft distribution and migration directionality exhibited AC frequency dependence in fibroblasts (Fig. 5*C*). Previous studies also described frequency-dependent surface protein polarization in AC EF (48).

Lipid rafts have been shown to mediate mechanotransduction through spatial or allosteric regulation of protein functions (37, 49). However, it is not clear what initially leads to the changes in raft organization. In this study, we demonstrate that lipid rafts are the primary sensing mechanism to external EF and regulate

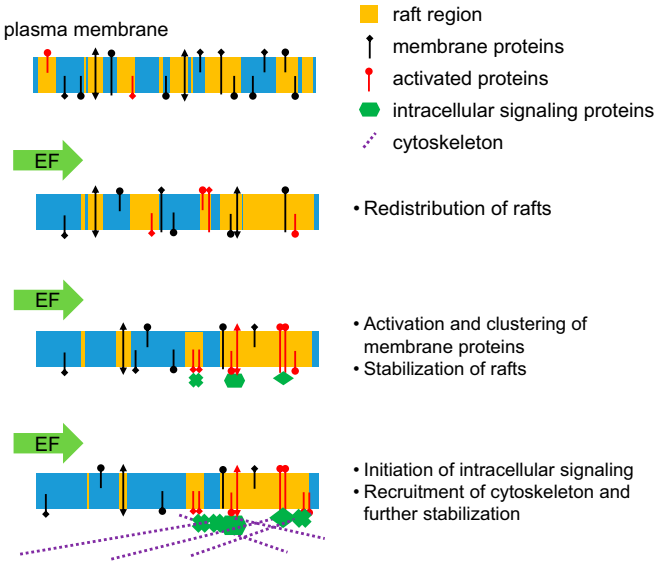

Fig. 6. Model of EF-induced lipid raft polarization and signaling. EF directs lipid raft polarization and the increased density of raft and the constituent proteins.

downstream protein signaling. A recent study reports that caveolae disassembles and reassembles in response to membrane stretch and relaxation, which can lead to raft reorganization (50). In addition, kinetic disruption of lipid rafts activates phospholipase D2 by mixing the enzyme with its substrate (51). These studies support our notion that lipid rafts play a principle role in mechanosensing. How does the interaction between lipid raft and scaffolding proteins influence raft dynamics in EF? For instance, EF stimulation increases oligomeric Cav content, which can be part of the curved caveolae structures or smaller Cav scaffolds (52). Although the oligomers are mostly associated with caveolae, noncaveolar Cav oligomers have also been reported (52). Further in-depth investigations using tools in protein and lipid dynamics and superresolution imaging will be needed to delineate the role of Cav and caveolae in integrin activation and EF-induced migration.

EF-induced migration has been described for over a century and is implicated in wound healing, development, and metastasis. Although the intracellular signaling machinery is similar to other cell migration mechanisms, the identity of a single critical macromolecule for sensing the field remains unknown. Using theoretical model and experimental results, we demonstrate that lipid rafts are the primary sensing element in EF-induced cell polarization and migration. As illustrated in Fig. 6, these membrane nanodomains act as mobile complexes that polarize, coalesce, and partition membrane proteins such as integrin and Cav. Raft, integrin, and Cav are all necessary for downstream intracellular signaling, including RhoA and PI3K, to polarize the cell for directed migration. Our findings establish a fundamental mechanism for cell electrosensing and provide a role in lipid raft mechanotransduction.

Methods and Materials

Detailed methods are described in *SI Appendix*.

Electrical Stimulation. The galvanotaxis chamber, as described previously (53), consisted of a modified parallel-plate flow chamber where the medium inlet and outlet were connected to agarose salt bridges. Constant DC EF was applied at a field strength of 6 V/cm (3 mA) with a Keithley SourceMeter, and AC sinusoid waves were applied at a peak intensity of 1.2 V at 50 Hz using a custom stimulator (Dynaprog).

Migration Analysis. Images of cell location were captured every 15 min on an inverted microscope (Leica). Cell migration was measured by manually determining the centroid with time and calculating the displacement and direction (angle between the EF direction and the cell translocation vector). Migration speed was calculated as the net displacement per hour, and migration directionality was calculated as the cosine of the migration angle where a negative value indicates migration toward the cathode.

Image Analysis. A custom LabView program (National Instruments) allowed manual selection of cell area (via the bright-field channel) and automated partition of four quadrants (Fig. 1*B*). The mean fluorescent intensity was calculated for each quadrant and normalized to overall cell intensity. Asymmetry index (AI) was calculated by subtracting the normalized intensity of the anodal quadrant from the cathodal quadrant (17). A positive AI value indicates a preferential anodal distribution of the labeled molecules, and a negative value of AI indicates cathodal distribution. For stimulated emission depletion (STED) images, a custom Matlab program segmented and measured raft sizes.

Cav Oligomerization Assay. A modified galvanotaxis chamber was made by adapting the parallel plate geometry in a 10-cm culture dish with PDMS molding. Cells were cultured overnight and stimulated for 1 h. To determine the degree of Cav oligomerization, total cell lysates harvested with RIPA buffer were denatured in gel loading buffer at 70 °C for 10 min (54). Proteins were separated via standard SDS/PAGE procedures and blotted on PVDF membrane. The whole membrane was probed with Cav-1 antibody (Cell Signaling), and bands above 250 kDa (representing Cav oligomers) and at 22 kDa (Cav monomers) were detected (54).

Membrane Modeling. When an EF is applied, three forces acted on lipid rafts (12, 43, 44): the electrical force due to an F_E (45), the hydrodynamic force resulting from the aqueous medium (F_{HA}) (46), and the drag force in membrane (F_{DM}) (47). Drift velocity of the lipid rafts can be obtained by expressing F_E, F_{HA}, and F_{DM} in the forms with lipid raft velocity, as shown in Eq. **1**:

$$\vec{V} = \frac{\frac{d(r)\varepsilon_0\varepsilon_r(\zeta_a - \zeta_{EOF})\vec{E}}{\eta_a}}{d(r)+g(r)}, \qquad [1]$$

where $d(r)$ and $g(r)$ are the drag coefficients associated with the hydrophilic portion in the aqueous phase and with the portion embedded in the membrane, respectively.

The drag coefficient $d(r)$ is related to the shape, size, and orientation of the hydrophilic portion with respect to the aqueous flow (45, 55) and was obtained by using COMSOL Multiphysics software. For the cylindrical hydrophilic portion with a height of 1 nm, the obtained $d(r)$ is 2×10^{-11} ln(r) + 5×10^{-10}. The hydrophobic portion-associated drag force coefficient, $g(r)$, can be obtained by using the Saffman–Delbrück approximation and is expressed below (55–57):

$$g(r) = \frac{4\pi\eta_m\left[1-\left(\frac{\epsilon^3}{\pi}\right)\ln\left(\frac{2}{\epsilon}\right)+\frac{c_1\epsilon^{b_1}}{(1+c_2\epsilon^{b_2})}\right]}{\ln\left(\frac{2}{\epsilon}\right)-\gamma+\frac{4\epsilon}{\pi}-\left(\frac{\epsilon^2}{2}\right)\ln\left(\frac{2}{\epsilon}\right)}, \quad \epsilon = \frac{2r\eta_a}{\eta_m},$$

where r is the lipid raft radius, $\gamma = 0.58$, $b_1 = 2.75$, $b_2 = 0.61$, $c_1 = 0.74$, and $c_2 = 0.52$. Detailed descriptions and definitions of additional symbols can be found in *SI Appendix*.

Statistical Analysis. SPSS 22 (IBM) was used to perform ANOVA with LSD post hoc tests ($\alpha = 0.05$). All results represent more than two separate cell preparations. Error bars represent SEMs.

ACKNOWLEDGMENTS. The authors thank the Technology Commons in College of Life Science and the Instrumentation Center sponsored by Ministry of Science and Technology as well as the Molecular Imaging Center of National Taiwan University for technical assistance. The authors especially acknowledge Dr. Tang-long Shen for his helpful suggestions, Mr. Chih-Wei Liu and Lun-Zhang Guo for their assistance in STED imaging, and Prof. Tzy-Rong Lin from National Taiwan Ocean University for permission to use the COMSOL software in his lab. This work was supported by Ministry of Science and Technology (MOST) Grants 105-2221-E-002-006 and 105-2628-E-002-015-MY3, and National Health Research Institute Grant NHRI-EX106-10411EI.

1. Bentrup F, Sandan T, Jaffe L (1967) Induction of polarity inFucus eggs by potassium ion gradients. *Protoplasma* 64:254–266.
2. Nuccitelli R, Erickson CA (1983) Embryonic cell motility can be guided by physiological electric fields. *Exp Cell Res* 147:195–201.
3. Chiang M, Robinson KR, Vanable JW, Jr (1992) Electrical fields in the vicinity of epithelial wounds in the isolated bovine eye. *Exp Eye Res* 54:999–1003.
4. Chao P-HG, Lu HH, Hung CT, Nicoll SB, Bulinski JC (2007) Effects of applied DC electric field on ligament fibroblast migration and wound healing. *Connect Tissue Res* 48: 188–197.
5. Rajnicek AM, Foubister LE, McCaig CD (2006) Temporally and spatially coordinated roles for Rho, Rac, Cdc42 and their effectors in growth cone guidance by a physiological electric field. *J Cell Sci* 119:1723–1735.
6. Vandenberg LN, Morrie RD, Adams DS (2011) V-ATPase-dependent ectodermal voltage and pH regionalization are required for craniofacial morphogenesis. *Dev Dyn* 240:1889–1904.
7. Zhao M, et al. (2006) Electrical signals control wound healing through phosphatidylinositol-3-OH kinase-gamma and PTEN. *Nature* 442:457–460.
8. Zhao M, Forrester JV, McCaig CD (1999) A small, physiological electric field orients cell division. *Proc Natl Acad Sci USA* 96:4942–4946.
9. Shimeld SM, Levin M (2006) Evidence for the regulation of left-right asymmetry in Ciona intestinalis by ion flux. *Dev Dyn* 235:1543–1553.
10. Song B, Zhao M, Forrester J, McCaig C (2004) Nerve regeneration and wound healing are stimulated and directed by an endogenous electrical field in vivo. *J Cell Sci* 117: 4681–4690.
11. Jaffe LF (1977) Electrophoresis along cell membranes. *Nature* 265:600–602.
12. McLaughlin S, Poo MM (1981) The role of electro-osmosis in the electric-field-induced movement of charged macromolecules on the surfaces of cells. *Biophys J* 34:85–93.
13. Allen GM, Mogilner A, Theriot JA (2013) Electrophoresis of cellular membrane components creates the directional cue guiding keratocyte galvanotaxis. *Curr Biol* 23: 560–568.
14. Pullar CE, et al. (2006) beta4 integrin and epidermal growth factor coordinately regulate electric field-mediated directional migration via Rac1. *Mol Biol Cell* 17: 4925–4935.
15. Zhao M, Bai H, Wang E, Forrester JV, McCaig CD (2004) Electrical stimulation directly induces pre-angiogenic responses in vascular endothelial cells by signaling through VEGF receptors. *J Cell Sci* 117:397–405.
16. Zhao M, Pu J, Forrester JV, McCaig CD (2002) Membrane lipids, EGF receptors, and intracellular signals colocalize and are polarized in epithelial cells moving directionally in a physiological electric field. *FASEB J* 16:857–859.
17. Tsai C-H, Lin B-J, Chao P-HG (2013) $\alpha 2\beta 1$ integrin and RhoA mediates electric field-induced ligament fibroblast migration directionality. *J Orthop Res* 31:322–327.
18. Mycielska ME, Djamgoz MBA (2004) Cellular mechanisms of direct-current electric field effects: Galvanotaxis and metastatic disease. *J Cell Sci* 117:1631–1639.
19. Finkelstein EI, Chao P-HG, Hung CT, Bulinski JC (2007) Electric field-induced polarization of charged cell surface proteins does not determine the direction of galvanotaxis. *Cell Motil Cytoskeleton* 64:833–846.
20. Rosetti CM, Mangiarotti A, Wilke N (2017) Sizes of lipid domains: What do we know from artificial lipid membranes? What are the possible shared features with membrane rafts in cells? *Biochim Biophys Acta* 1859:789–802.
21. Vicidomini G, et al. (2015) STED-FLCS: An advanced tool to reveal spatiotemporal heterogeneity of molecular membrane dynamics. *Nano Lett* 15:5912–5918.
22. Leitinger B, Hogg N (2002) The involvement of lipid rafts in the regulation of integrin function. *J Cell Sci* 115:963–972.
23. Casalou C, et al. (2011) Cholesterol regulates VEGFR-1 (FLT-1) expression and signaling in acute leukemia cells. *Mol Cancer Res* 9:215–224.
24. Zhu D, Xiong WC, Mei L (2006) Lipid rafts serve as a signaling platform for nicotinic acetylcholine receptor clustering. *J Neurosci* 26:4841–4851.
25. Rey-Barroso J, et al. (2013) The dioxin receptor controls $\beta 1$ integrin activation in fibroblasts through a Cbp-Csk-Src pathway. *Cell Signal* 25:848–859.
26. Pelkmans L, Bürli T, Zerial M, Helenius A (2004) Caveolin-stabilized membrane domains as multifunctional transport and sorting devices in endocytic membrane traffic. *Cell* 118:767–780.
27. Sun Y-S, Peng S-W, Lin K-H, Cheng J-Y (2012) Electrotaxis of lung cancer cells in ordered three-dimensional scaffolds. *Biomicrofluidics* 6:14102–1410214.
28. Finkelstein E, et al. (2004) Roles of microtubules, cell polarity and adhesion in electric-field-mediated motility of 3T3 fibroblasts. *J Cell Sci* 117:1533–1545.
29. Gowrishankar K, et al. (2012) Active remodeling of cortical actin regulates spatiotemporal organization of cell surface molecules. *Cell* 149:1353–1367.
30. Raghupathy R, et al. (2015) Transbilayer lipid interactions mediate nanoclustering of lipid-anchored proteins. *Cell* 161:581–594.
31. Saha S, et al. (2015) Diffusion of GPI-anchored proteins is influenced by the activity of dynamic cortical actin. *Mol Biol Cell* 26:4033–4045.
32. Kusumi A, Suzuki K (2005) Toward understanding the dynamics of membrane-raft-based molecular interactions. *Biochim Biophys Acta* 1746:234–251.
33. Yang B, Radel C, Hughes D, Kelemen S, Rizzo V (2011) p190 RhoGTPase-activating protein links the $\beta 1$ integrin/caveolin-1 mechanosignaling complex to RhoA and actin remodeling. *Arterioscler Thromb Vasc Biol* 31:376–383.
34. Roy S, et al. (1999) Dominant-negative caveolin inhibits H-Ras function by disrupting cholesterol-rich plasma membrane domains. *Nat Cell Biol* 1:98–105.
35. Siegel AP, Kimble-Hill A, Garg S, Jordan R, Naumann CA (2011) Native ligands change integrin sequestering but not oligomerization in raft-mimicking lipid mixtures. *Biophys J* 101:1642–1650.
36. Salani B, et al. (2009) IGF-I induced rapid recruitment of integrin $\beta 1$ to lipid rafts is Caveolin-1 dependent. *Biochem Biophys Res Commun* 380:489–492.
37. Sun X, et al. (2016) Activation of integrin $\alpha 5$ mediated by flow requires its translocation to membrane lipid rafts in vascular endothelial cells. *Proc Natl Acad Sci USA* 113:769–774.
38. Gaus K, Le Lay S, Balasubramanian N, Schwartz MA (2006) Integrin-mediated adhesion regulates membrane order. *J Cell Biol* 174:725–734.
39. Zhao M, Dick A, Forrester JV, McCaig CD (1999) Electric field-directed cell motility involves up-regulated expression and asymmetric redistribution of the epidermal growth factor receptors and is enhanced by fibronectin and laminin. *Mol Biol Cell* 10: 1259–1276.
40. Wary KK, Mariotti A, Zurzolo C, Giancotti FG (1998) A requirement for caveolin-1 and associated kinase Fyn in integrin signaling and anchorage-dependent cell growth. *Cell* 94:625–634.
41. Cao H, Courchesne WE, Mastick CC (2002) A phosphotyrosine-dependent protein interaction screen reveals a role for phosphorylation of caveolin-1 on tyrosine 14: Recruitment of C-terminal Src kinase. *J Biol Chem* 277:8771–8774.
42. Tatton L, Morley GM, Chopra R, Khwaja A (2003) The Src-selective kinase inhibitor PP1 also inhibits Kit and Bcr-Abl tyrosine kinases. *J Biol Chem* 278:4847–4853.
43. Yoshina-Ishii C, Boxer SG (2006) Controlling two-dimensional tethered vesicle motion using an electric field: Interplay of electrophoresis and electro-osmosis. *Langmuir* 22: 2384–2391.
44. Han X, et al. (2009) Manipulation and charge determination of proteins in photopatterned solid supported bilayers. *Integr Biol* 1:205–211.
45. Bier M (1959) *Electrophoresis: Theory, Methods, and Applications* (Academic, New York).
46. Bird BR, Stewart WE, Lightfoot EN (1960) *Transport Phenomena* (Wiley, New York).
47. Petrov EP, Schwille P (2008) Translational diffusion in lipid membranes beyond the Saffman-Delbruck approximation. *Biophys J* 94:L41–L43.
48. Cho MR, Thatte HS, Lee RC, Golan DE (1994) Induced redistribution of cell surface receptors by alternating current electric fields. *FASEB J* 8:771–776.
49. Mitchell JS, Brown WS, Woodside DG, Vanderslice P, McIntyre BW (2009) Clustering T-cell GM1 lipid rafts increases cellular resistance to shear on fibronectin through changes in integrin affinity and cytoskeletal dynamics. *Immunol Cell Biol* 87:324–336.
50. Sinha B, et al. (2011) Cells respond to mechanical stress by rapid disassembly of caveolae. *Cell* 144:402–413.
51. Petersen EN, Chung H-W, Nayebosadri A, Hansen SB (2016) Kinetic disruption of lipid rafts is a mechanosensor for phospholipase D. *Nat Commun* 7:13873.
52. Lajoie P, Goetz JG, Dennis JW, Nabi IR (2009) Lattices, rafts, and scaffolds: Domain regulation of receptor signaling at the plasma membrane. *J Cell Biol* 185:381–385.
53. Tandon N, et al. (2009) Electrical stimulation systems for cardiac tissue engineering. *Nat Protoc* 4:155–173.
54. Sargiacomo M, et al. (1995) Oligomeric structure of caveolin: Implications for caveolae membrane organization. *Proc Natl Acad Sci USA* 92:9407–9411.
55. Peters R, Cherry RJ (1982) Lateral and rotational diffusion of bacteriorhodopsin in lipid bilayers: Experimental test of the Saffman-Delbrück equations. *Proc Natl Acad Sci USA* 79:4317–4321.
56. Guigas G, Weiss M (2008) Influence of hydrophobic mismatching on membrane protein diffusion. *Biophys J* 95:L25–L27.
57. Saffman PG, Delbrück M (1975) Brownian motion in biological membranes. *Proc Natl Acad Sci USA* 72:3111–3113.